



Design, Structural Characterization, Molecular docking and Biomedical Applications Of Hydrazone-based Schiff base Metal Complexes



CrossMark

Emam M. Komyha, Walaa H. Mahmoud, Wafaa M. Hosny, Ahmed A. El-Sherif*

Department of Chemistry, Faculty of Science, Cairo University, Egypt

Abstract

newly synthesized Schiff base ligand, (E)-N'-((E)-1-(2-(p-tolyl)hydrazono)propan-2-ylidene)benzohydrazide, was used to design six mononuclear metal chelated complexes. Several methods, including CHN analysis, infrared, proton nuclear magnetic resonance, mass spectrum analysis, and conductivity tests, were used to fully analyze the chemical structures of the produced compounds. Using a 2,2-diphenyl-2-picryl-hydrazyl free radical scavenging assay, the antioxidant activity of the metal complexes against active free radicals was identified. All compounds were also tested for their ability as antibacterial, antifungal, and anticancer. It was concluded during preliminary in vitro antibacterial and antifungal screening activities that the complexes had greater activity against the tested strains than did the free ligand. With a very low IC₅₀ (1.537 µg/ml), the Mn(II) compound demonstrated promising efficiency against HepG2 cells. The binding of the Schiff base ligand (L) with several protein receptors was predicted using molecular docking. The docking study provides useful structural data for the results of the inhibition investigation.

Keywords: Schiff base complexes; antimicrobial; anticancer; antioxidant; molecular docking.

1. Note

Considering their biological characteristics (such as anticancer and antibacterial), Schiff bases are among the organic compounds that are thought to play a significant role in the pharmaceuticals industry [1, 2]. They are widely used in several sectors. They can function as catalysts for a variety of organic redox reactions, high-inhibition anticorrosion agents, organic semiconductors, filaments, deodorants, light stabilizers, dental materials, cross-linked polymers, and fragrances [3-5]. Schiff bases can participate in complex formation by contributing their lone pairs of electrons for stability, which is also reliant on the substitution groups on the compounds. This is

made possible by the existence of heterocyclic nitrogen, oxygen, and sulfur atoms. Due to their readily available preparation methods and diverse structural makeup, Schiff base complexes with transition metals are suggested as the primary stereochemical models in coordination chemistry [6,7]. As biochemical, analytical, and antibacterial reagents, they are becoming increasingly important [8-12].

A major contribution to the synthesis of metal-ligand bonds is also contributed by the lone pair of electrons that are available on heteroatoms. Due to their extraordinary capacity for building complexes and extensive use as spectrometric and gravimetric reagents in analytical chemistry, Schiff base ligands with N, O, and S donor atoms have drawn a lot of attention over the years. Additionally, it has been claimed that

*Corresponding author e-mail: aelsherif@sci.cu.edu.eg / aelsherif72@yahoo.com (Ahmed El-Sherif)

Received date 2022-07-31; revised date 2023-04-13; accepted date 2023-05-25

DOI: 10.21608/EJCHEM.2023.147796.6650

©2023 National Information and Documentation Center (NIDOC)

administering these chemicals as metal complexes increases their action [12-16].

In the current study, a bidentate Schiff base ligand [L] and its M(III)/(II) complexes were developed and characterized utilizing analytical methods such as CHN analysis, UV-Vis spectroscopy, FT-IR spectroscopy, ^1H NMR, EI-mass spectral analysis, and conductivity measurements. This study's primary goal is to demonstrate that the synthesized compounds are strong competitors for diverse biomedical applications by analyzing the coordination properties of the novel Schiff base with various M(II)/(III) [17,18].

Materials and methods

Experimental

2.1.1. Chemicals and reagents

The (*E*)-1-(2-(*p*-tolyl)hydrazono)propan-2-one and benzohydrazide were purchased from the Merck group. The metal salts $\text{CrCl}_3 \cdot 6\text{H}_2\text{O}$, $\text{MnCl}_2 \cdot 2\text{H}_2\text{O}$, $\text{CoCl}_2 \cdot 6\text{H}_2\text{O}$, $\text{NiCl}_2 \cdot 6\text{H}_2\text{O}$, $\text{CuCl}_2 \cdot 2\text{H}_2\text{O}$ (Sigma-Aldrich), and K_2PdCl_4 (Merck) were also obtained from the Merck group. Absolute ethanol and dimethyl formamide (DMF) were employed as organic solvents. All of the chemical utilized was provided in the highest purity attainable and all preparations were prepared using deionized water. The American Type Culture Collection provided both the human liver cancer (HepG2) and prostate tumor cell line (PC3), which were received frozen in liquid nitrogen (-180°C). The National Cancer Institute in Cairo, Egypt, used serial sub-culturing to maintain the tumor cell lines.

2.1.2. Solutions

For conductivity experiments, metal complex solutions (1×10^{-3} M) have been synthesized in DMF [19,20]. The Schiff base ligand and its complexes were obtained in 1×10^{-4} M solutions for UV-Vis spectral measurements.

2.1.3. Instrumentation

A CHNS-932 (LECO) Vario Elemental analyzer at the Microanalytical Center, Cairo University, Egypt was used to perform microanalysis of carbon, hydrogen, and nitrogen. The melting point was determined using triforce

XMTD-3000. The Fourier transform infrared (FT-IR) spectra were obtained using (Perkin-Elmer, 1650 spectrometer), and KBr disks within the range of $4000\text{--}400\text{ cm}^{-1}$. ^1H NMR spectra were recorded at ambient temperature using a 300-MHz Varian-Oxford, Mercury, in dimethyl sulfoxide-*d*₆ (DMSO-*d*₆) solutions and tetramethylsilane that serve as an internal standard. The magnetic susceptibilities of powdered samples were calculated using the Faraday method.

The molar conductance of solid complex solutions in ethanol at concentrations of 10^{-3} M was determined using a Jenway 4010 conductivity meter. MS-5988 GS-MS Hewlett-Packard instrument was used to acquire mass spectra through the electron ionization method at 70 eV. A UV-Vis Perkin-Elmer Model Lambda 20 automated spectrophotometer was used to give the spectrum of solutions at wavelengths between 200 and 700 nm.

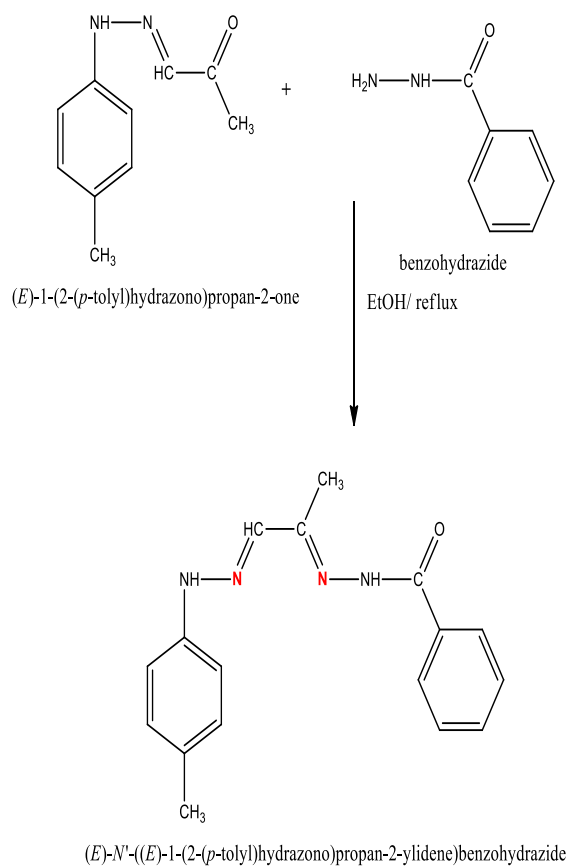
The research on antimicrobial and anticancer activities was conducted at the Microanalytical Center, and the National Cancer Institute, Cancer Biology Department, and Pharmacology Department, Cairo University, respectively. A microplate reader (Meter Tech. R960, USA) was used to spectrophotometrically measure the enzyme-linked immunosorbent assay (ELISA) at 564 nm. The central labs of the Faculty of Agriculture, Cairo University were employed to assess the antioxidant activity.

1.1. procedures

Synthesis of the Schiff base ligand [L]

According to the suggested technique, a novel Schiff base ligand was synthesized. This was accomplished by condensing benzohydrazide (5 mmol, 0.68 g), which was dissolved in hot 100% ethanol (60°C), and (*E*)-1-(2-(*p*-tolyl)hydrazono)propan-2-one (5 mmol, 0.88 g), which was dissolved in hot ethanol in a 1:1 molar ratio. The reaction mixture was then placed in reflux for 4 hours.

Subsequently, an orange solid compound was isolated from the DMF-ethanol mixture, filtered out, and recrystallized to produce a pure Schiff base with a yield of 89%. The structure and general formation reaction of the Schiff base ligand are shown in Scheme (1).



Scheme. 1: Synthesis pathway of the Schiff base ligand (L).

1.1.1.

Synthesis of the metal complexes

The metal complexes were synthesized by combining a hot ethanolic solution (70°C) of the Schiff base ligand (1.7 mmol, 0.5 g) within a hot absolute ethanol (20 ml) solution of metal salts (0.85-mmol, 0.23-g $\text{CrCl}_3 \cdot 6\text{H}_2\text{O}$, 0.17-g $\text{MnCl}_2 \cdot 2\text{H}_2\text{O}$, 0.23-g $\text{CoCl}_2 \cdot 6\text{H}_2\text{O}$, 0.23-g $\text{NiCl}_2 \cdot 6\text{H}_2\text{O}$, 0.14-g $\text{CuCl}_2 \cdot 2\text{H}_2\text{O}$, and 0.27-g K_2PdCl_4). After 3 hours of stirring in reflux, the resultant complexes began to precipitate from the mixtures. The precipitates were collected by filtration, cleaned by repeated washings, and dried under a vacuum over anhydrous calcium chloride. Consequently, the pure metal Complexes resulted through the recrystallization process.

1.2. Antimicrobial activity

The disc diffusion technique was used to assess the in vitro antibacterial and antifungal properties of gentamycin, ampicillin, and amphotericin B, which served as positive controls for Gram-positive, Gram-negative bacteria, and

fungi, respectively [21, 22]. The bacterial organisms used were Gram-positive bacteria (*Bacillus subtilis*, *Bacillus cereus*, and *Staphylococcus aureus*), Gram-negative bacteria (*Escherichia coli*, *Pseudomonas aeruginosa*, and *Neisseria gonorrhoeae*), and fungal strains (*Candida albicans* and *Aspergillus flavus*). The Schiff base ligand and its complexes were dissolved in DMSO to prepare the stock solutions (1 mmol). For the antibacterial activity assessment, a nutrient agar medium was prepared, cooled to 47°C, and seeded with microorganisms. After the material had solidified, a sterile cork borer was used to drill 5-mm-diameter holes. The investigated compounds (the Schiff base ligand and its metal complexes) after being dissolved in DMSO at 1×10^{-3} M were added to Petri dishes (only 0.1 ml). The growth plates of bacteria and fungi were then placed in an incubator for 20 hours at 37°C. Then the inhibition zones were subjected to diameter measurements in millimeters. The average of the final reading of antimicrobial activity assessments was determined by carrying out the antimicrobial activity experiments in triplicate [23].

1.3. Antitumor activity

The Skehan and Storeng method was used to examine the possible cytotoxicities of synthesized compounds [24]. Before treatment with the compounds, cells were plated in a 96-multiwell plate with 104 cells per well for 24 h to allow the cell to adhere to the plate wall. For each dose, triplicate wells were made and three different concentrations of the chemicals (0, 5, 12.5, 25, 50, and 100 $\mu\text{g}/\text{mL}$) were applied to the cell monolayer. The compounds with the monolayer cells were incubated at 37°C and in a 5% CO_2 atmosphere for 48 hours. Afterward, the cells were fixed, cleaned, and stained with the sulforhodamine B stain after 48 hours. Acetic acid was used to wash away the excess stain, while the Tris-EDTA buffer was used to recover the adhered stain. An ELISA microplate reader was used to detect the OD of each well spectrophotometrically at 564 nm. The mean background absorbance was automatically subtracted, and the average values of each drug concentration were calculated. To determine the breast tumor cell line survival curve for each compound, the relationship between the surviving fraction and drug concentration was plotted. Following is the formula used to determine the cell survival percentage:

$$\text{Survival fraction} = \frac{\text{OD (treated cells)}}{\text{OD (control cells)}}$$

The experiment was carried out three times to get the IC₅₀ values (the concentrations of the [L] ligand or its complexes required to elicit 50% cell growth inhibition).

1.4. In vitro antioxidant activity

Using ascorbic acid as a reference standard material, the 1,1-diphenyl-2-picrylhydrazyl test was used to evaluate the synthesized compounds' capacity to scavenge free radicals [25]. A Thermo Scientific Evolution 201 UV-Visible Spectrometer was used to measure the absorbances of the sample, blank, and control in the dark at 517 nm. Three different experimental tests were conducted. The proportion of antioxidant activity was calculated as follows:

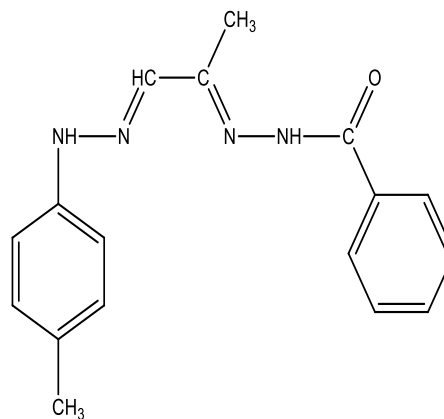
$$\text{Antioxidant activity percentage} = 100 - \left[\frac{(Abs_{\text{sample}} - Abs_{\text{blank}}) \times 100}{Abs_{\text{control}}} \right]$$

1.5. Molecular docking

The crystal structures of *S. aureus*' nucleoside diphosphate kinase (3Q8U), *E. coli*'s protein phosphatase (3t88), and the fungus *C. albicans*' protein phosphatase (5JPE) were used to anticipate the potential binding modes of the most active drugs with these receptors. Additionally, these investigations were carried out to determine the inhibitor's binding free energy inside the macromolecule [26,27]. In order to calculate and present an interactive molecular graphics program, the potential docking modes of a receptor and a Schiff base ligand molecule were carried out using the MOE 2008 software (MOE source: Chemical Computing Group Inc., Quebec, Canada, 2008). It required inputs in PDB format for the ligand and the receptor. The co-crystallized ligands, water molecules, and other unsupported substances (such as Na, K, and Hg) were eliminated while the amino acid chain was preserved. Gaussian03 software was used to construct the Schiff base ligand structure in a PDB file format. From the Protein Data Bank (<https://www.rcsb.org>), the crystal structures of the various receptors were retrieved.

2. Results and Discussion

The newly synthesized L Schiff base ligand (*E*)-*N'*-((*E*)-1-(2-(*p*-tolyl)hydrazono)propan-2-ylidene)benzohydrazide underwent elemental analysis, electron ionization-mass spectrometry (EI-MS), IR, UV-Vis, and ¹H NMR spectrum studies. The findings of the elemental analyses (C, H, and N) are in good agreement with the formulas suggested in Table 1 and Fig. 1.



(*E*)-*N'*-((*E*)-1-(2-(*p*-tolyl)hydrazono)propan-2-ylidene)benzohydrazide

Figure. 1: Structure of Schiff base ligand (L).

The purity of the Schiff base ligand (L) was demonstrated by its sharp melting point. The distinctive stretching vibration bands for the L ligand can be seen in the IR data (Table 2) at 1598, 1627, and 3263 cm⁻¹ for the $\nu(\text{C}=\text{N})$ azomethine, $\nu(\text{CO})$, and $\nu(\text{NH})$ groups, respectively [28–30].

The characteristic proton signals could be seen in the ¹H NMR spectra of the isolated L-free ligands recorded in DMSO-*d*₆ at room temperature (Table 3). In addition to another singlet signal at 7.49 ppm attributable to an azomethine proton, two signals emerged at 10.64 and 10.58 ppm and were characteristic of two separate NH protons of the L free ligand (exchangeable with D₂O) [31].

A recording of the Schiff base ligand's mass spectrum was presented. The resulting molecular ion (m/z) peak at 294 amu supported the proposed formulation, in which the ligand moiety was C₁₇H₁₈N₄O. In addition, several peaks in the mass spectrum were shown that each one corresponding to a different stage in the ligand's breakdown.

2.1. Elemental analyses and molar conductivity measurements

The complexes of Cr(III), Mn(II), Co(II), Ni(II), Cu(II), and Pd(II) are all air-stable. In real life, they are largely soluble in polar organic solvents including EtOH, MeOH, DMF, and DMSO. They cannot dissolve in water, though. Additionally, elemental analysis was used to corroborate the stoichiometry and formulation of the Schiff base (L) ligand and its metal complexes which were confirmed to have a metal/ligand ratio of 1:2 in the complexes. This was done by measuring the metal contents of the complexes as well as their carbon, hydrogen, nitrogen, and chlorine contents (Table 1). The ligand and their

complexes' elemental studies show good agreement with the suggested structures. It was observed that the molar conductivity (Λ_m) values of metal complexes in DMF (10^{-3} M) at 25 °C ranged from 18 to 115 $\Omega^{-1} \text{ mol}^{-1} \text{ cm}^2$, indicating that the complexes of Ni(II), Cu(II), and Pd(II) were ionic in nature and 1:2 electrolytes, while Cr(III) was a 1:1 electrolyte. The low molar conductance values of 18 and 41 $\Omega^{-1} \text{ mol}^{-1} \text{ cm}^2$ for the Mn(II) and Co(II) complexes, respectively, indicate that they are non-electrolytic [32]. This suggested that the coordination sphere was where the anions were found. Table 1 presents the findings.

Table 1: Physical and analytical data of Schiff base ligand (L) and its metal complexes

Compound (chemical formula)	Color Yield (%)	M.p. (°C)	Found (Calcd)				μ_{eff} (BM)	Λ_m ($\Omega^{-1} \text{ mol}^{-1} \text{ cm}^2$)
			C (%)	H (%)	N (%)	M (%)		
L ($\text{C}_{17}\text{H}_{18}\text{N}_4\text{O}$)	orange (89)	185	69.28 (69.38)	6.05 (6.12)	18.98 (19.04)	—	—	—
$[\text{Cr}(\text{L})_2\text{Cl}_2]\text{Cl}$	Brown (92)	105	54.27 (54.66)	4.32 (4.82)	14.91 (15.03)	6.48 (6.97)	3.22	76
$[\text{Mn}(\text{L})_2\text{Cl}_2]$	Brown (87)	196	56.69 (56.90)	4.96 (5.04)	15.30 (15.62)	7.64 (7.70)	5.56	18
$[\text{Co}(\text{L})_2\text{Cl}_2]$	Brown (95)	150	56.70 (56.82)	4.95 (5.01)	15.54 (15.59)	8.11 (8.21)	5.03	41
$[\text{Ni}(\text{L})_2] \text{Cl}_2$	Brown (93)	193	56.72 (56.90)	4.90 (5.02)	15.48 (15.62)	7.89 (8.08)	2.97	103
$[\text{Cu}(\text{L})_2] \text{Cl}_2$	Brown (91)	> 300	56.02 (56.44)	4.59 (4.98)	15.26 (15.49)	8.36 (8.72)	1.82	115
$[\text{Pd}(\text{L})_2] \text{Cl}_2$	Pale yellow (80)	195	53.20 (53.31)	4.35 (4.70)	14.46 (14.63)	13.68 (13.90)	Dia.	109

2.2. FT-IR spectral data

A KBr pellet was used to record the vibrational spectra of the produced compounds in the 4000-400 cm^{-1} range, and the results are shown in Table 2. Comparing the infrared spectra of the parent ligand and the corresponding metal complexes allows one to investigate the coordination mechanism of the ligand toward the metal centers. The azomethine group in this study displayed a distinctive strong band at 1598 cm^{-1} , which is shifted in the complexes to 1580-1620 cm^{-1} , showing that coordination occurred through the nitrogen atom of the azomethine groups [26-28]. Moreover, due to the presence of NH groups, the

complexes produced a sharp band at 3314-3440 cm^{-1} . Additionally, all complexes exhibited nonligand bands in the range of 421-503 cm^{-1} , greatly corroborating the idea that coordination took place via the nitrogen atoms in the azomethine [33, 36].

2.3. ^1H NMR spectra

Table 3 contains the ^1H NMR spectra of the ligand and its Pd(II) complex. Two signals from the NH resonance can be seen in the ^1H NMR spectra of both molecules at 10.64 and 10.58 ppm for the free L and 10.62 and 10.48 ppm for the Pd(II)-L complex, proving that the two amine environments are not equivalent. The coordination of the imine nitrogen to metal centers is demonstrated by the shifting of the imine signals for the Pd(II) complex. Both the free L and its Pd(II) complex showed several signals for the aromatic protons [37].

2.4. Mass spectra

the EI-MS technique was used in this work to corroborate the mass of the ligand [38] L and its complexes by examining the intense molecular ion peaks in the spectra shown at $m/z = 294$ $[\text{M}]^+$ (L), 747 $[\text{M}+1]^+$ (Cr complex), 714 $[\text{M}]^+$ (Mn complex), 718 $[\text{M}-1]^+$ (Co complex), 718 $[\text{M}]^+$ (Ni complex), 723 $[\text{M}+1]^+$ (Cu complex), and 766 $[\text{M}+1]^+$ (Pd complex). The molecular ions results confirmed that the 1:2 metal-to-ligand stoichiometric ratio obtained from the EI-MS data is adequate.

Table 3: ¹H NMR spectral data of the Schiff base ligand (L) and its Pd(II) complex

Compound	Chemical shift, (δ) ppm	Assignment
L	10.64	(s, H, NH-CO)
	10.58	(s, H, NH)
	7.49	(s, H, azomethine CH)
	7.52-7.86	(m, 5H, aromatic)
	6.95-7.07	(m, 4H, aromatic)
	2.24	(s, 3H, ph-CH ₃)
	2.22	(s, 3H, CH ₃)
[Pd(L) ₂]Cl ₂	10.62	(s, H, NH-CO)
	10.48	(s, H, NH)
	7.52	(s, H, azomethine CH)
	7.57-7.80	(m, 5H, aromatic)
	6.94-7.11	(m, 4H, aromatic)
	2.26	(s, 3H, ph-CH ₃)
	2.21	(s, 3H, CH ₃)

Candida albicans exhibited strong antifungal activity in the Co(II) and Ni(II) metal complexes (Table 4). According to the overall findings, the synthesized Co complex was more effective than the parent ligand and the other complexes against various bacterial and fungal species. Based on the chelation theory, the enhanced antibacterial and antifungal activity of the produced metal Schiff base complexes presented here can be adequately explained [43].

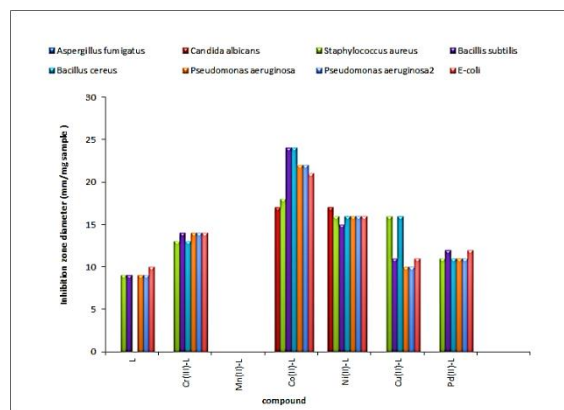


Figure 2: Biological activity of Schiff base ligand and its metal complexes against different bacterial and fungal species.

2.5. UV-Vis spectral study

The parent ligand and its complexes' UV-Vis absorption spectra were studied in the 200–900 nm range in the room-temperature DMF solution. The ligand's spectrum exhibits strong bands at 257, 308, and 368 nm in the ultraviolet region. The π - π^* and n - π^* intramolecular transitions of the ligand are responsible for these bands [32, 33]. Furthermore, as a result of their coordination with metal ions in the ranges of 242–266, 265–307, and 358–370 nm, respectively, these bands were shifted in all complexes.

2.6. Antimicrobial activity

The disc diffusion method was used to test the synthesized ligand and its metal(II)/(III) complexes for antibacterial and antifungal activity against some Gram-positive (*B. cereus*, *B. subtilis*, and *S. aureus*) and Gram-negative (*E. Coli*, *N. gonorrhoeae*, and *P. aeruginosa*) bacterial strains as well as (*A. flavus* and *C. albicans*) (Fig. 2). The observations of antibacterial and antifungal activities are listed in Table 4. The observed outcomes demonstrate the present analysis's complexes' efficacy against both Gram-positive and Gram-negative bacterial strains [41,42]. Only

2.7. Anticancer activity

The cytotoxicity of the produced complexes against the human hepatoma cell line (HepG2) and prostate cancer cell line (PC3) was used to evaluate their anticancer properties. The MTT colorimetric test was used to determine significant cytotoxicity and anticancer activity against HepG2 and PC3 cells after a 24-hour incubation (Table 5). The complexes' anticancer impact was concentration-dependent. As the complexes' concentrations increased, the viability of the cells decreased. Notably, the complexation of the ligand with the metal particles increased the anticancer action [44–46]. The highest significant cytotoxicity against HepG2 was reported by the Mn(II), Ni(II), and Pd(II) complexes. The IC₅₀ for the Mn(II) compound against HepG2 was extremely low. While the Ni(II) complex displayed the strongest activity and the lowest IC₅₀ towards the PC3 cell line, (Fig. 3).

Table 4: Biological activity of L ligand and its metal complexes

Sample		Inhibition zone diameter (mm / mg sample)							
		Gram-positive bacterial species			Gram-negative bacterial species			Fungi	
		<i>Bacillus cereus</i>	<i>Bacillus subtilis</i>	<i>Staphylococcus aureus</i>	<i>E.coli</i>	<i>Neisseria gonorrhoeae</i>	<i>Pseudomonas aeruginosa</i>	<i>Aspergillus flavus</i>	<i>Candida albicans</i>
L		NA	9	9	10	9	9	NA	Na
[Cr(L) ₂ Cl ₂]Cl		13	14	13	14	13	14	NA	NA
[Mn(L) ₂ Cl ₂]		NA	NA	NA	NA	NA	NA	NA	NA
[Co(L) ₂ Cl ₂]		24	24	18	21	20	22	NA	17
[Ni(L) ₂] Cl ₂		16	15	16	16	15	16	NA	17
[Cu(L) ₂] Cl ₂		16	11	10	11	10	10	NA	NA
[Pd(L) ₂] Cl ₂		11	12	11	12	10	11	NA	NA
Standard	Ampicillin	26	26	21	25	28	26	----	----
	Amphotericin B	----	----	----	----	----	----	17	21

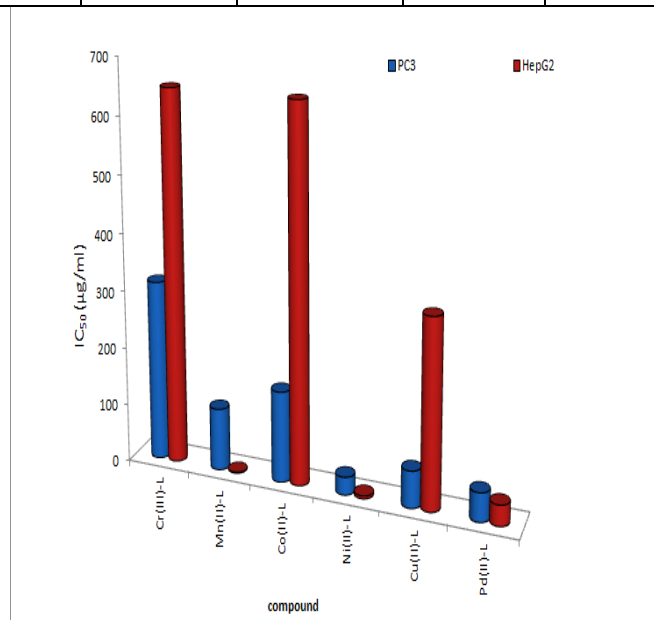
NA: no activity

Ampicillin: Standard antibacterial agent;

Amphotericin B: Standard antifungal agent.

Table 5: Anti-breast cancer activity of L ligand and its metal complexes against prostate cancer cell line (PC3) and liver cancer cell line (HepG2)

Compound	IC ₅₀ (μg/ml)	
	PC3	HepG2
[Cr(L) ₂ Cl ₂]Cl	314.4	648.7
[Mn(L) ₂ Cl ₂]	108.3	1.537
[Co(L) ₂ Cl ₂]	157.9	649.8
[Ni(L) ₂] Cl ₂	30.83	5.09
[Cu(L) ₂] Cl ₂	63.56	326.7
[Pd(L) ₂] Cl ₂	49.64	36.18

Figure 3: IC₅₀ of Schiff base (L) with prostate (PC3) and liver (HepG2) cancer cell lines.

2.8. Antioxidant activity

The ability of the produced metal complexes to act as antioxidants was tested using the 2,2-diphenyl-2-picryl-hydrazyl (DPPH•) free radical scavenging method. All metal complexes' antioxidant activity is shown in Fig. 4. The DPPH solution containing odd electrons demonstrated a prominent absorption band at 517 nm in the UV-Vis spectroscopy during the antioxidant activity testing. In its solution state, the stable DPPH• radical was a rich shade of violet. The DPPH• radical was neutralized and changed into 1,1-diphenyl-2-picryl-hydrazine when combined with the metal complexes (antioxidants), as demonstrated by the deep violet solution turning pale yellow. The reduction in its absorbance value at 517 nm can be used to calculate the antioxidant capability. The DPPH• free radical's % scavenging activity was calculated using the formula below: Scavenging activity percentage (%) = $A_o - A_e / A_o \times 100$. The absorbances of DPPH in the presence and absence of antioxidants (metal complexes) are designated as A_o and A_e , respectively [38]. In this study, the metal complex activity was reported in terms of IC_{50} values, and the free radical scavenging activity increased with increasing metal complex concentrations [46]. The greater antioxidant activity of the metal complexes is shown by smaller IC_{50} values. According to the IC_{50} values, the Cr(III) complex has stronger antioxidant activity than other complexes and the free ligand (Table 6).

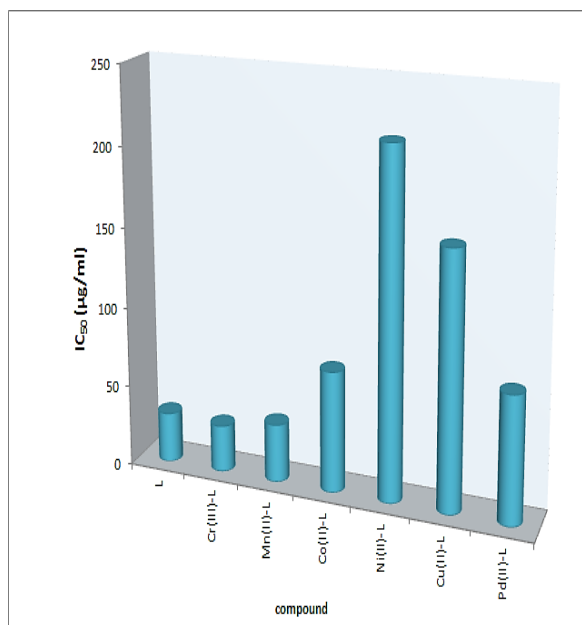


Figure 4: Antioxidant activity of L Schiff base ligand and its complexes.

Table 6: Antioxidant activity (DPPH free radical scavenging activity) of L ligand and its metal complexes

Compound	RSA%				IC ₅₀ (µg/ml)
	Concentration (µg/ml)				
	40	80	160	220	-----
L	63.7 4	71.9 3	74.8 5	75.96	31.38
[Cr(L) ₂ Cl ₂] Cl	68.4 8	78.0 1	83.8 0	86.6 1	29.21
[Mn(L) ₂ Cl ₂]	54.9 1	56.9 6	69.9 4	72.5 1	36.42
[Co(L) ₂ Cl ₂]	42.8 1	53.1 0	66.4 9	66.7 3	75.33
[Ni(L) ₂] Cl ₂	40.9 9	42.5 7	44.9 7	51.0 5	215.48
[Cu(L) ₂] Cl ₂	35.3 2	40.9 4	50.1 8	52.9 8	159.43
[Pd(L) ₂] Cl ₂	45.6 7	50.3 5	63.0 4	64.3 3	79.44

2.9. Docking

To show the binding affinity between these receptors and the ligand molecule, the Schiff base (L) was docked into the crystal structures of *Staphylococcus aureus* (3Q8U), *E. coli* (3t88), and the fungus *C. albicans* (5JPE) (Table 7). The H-bonding interactions were primarily responsible for the formation of the protein receptors' active sites that were drawn to L [40, 47]. The 5jpe receptor on *S. aureus* bacteria demonstrates strong binding energies for the L molecule (around -3.4 kcal/mol), according to the results of molecular docking (Fig. 5). Fig. 6 depicts the L compound's 2D and 3D molecular interactions.

Table 7: Interaction energy values obtained from docking calculations of L ligand with receptors of the crystal structure of nucleoside diphosphate kinase of *Staphylococcus aureus* (3Q8U) and crystal structure of *E. coli* (3T88) and protein phosphatase of fungus *Candida albicans* (5JPE)

Receptor	Ligand moiety	Receptor site	Interaction	Distance (Å)	E (kcal/mol)
5JPE	O 29	NH ₂ ARG 261 (A)	H-acceptor	2.86	-2.7
	O 29	NE2 HIS 290 (A)	H-acceptor	2.87	-2.8
	6 ring	CG2 VAL 298 (A)	pi-H	4.35	-0.7
3Q8U	N 21	NH ₂ ARG 102 (C)	H-acceptor	3.37	-3.4
	O 29	ND2 ASN 112 (C)	H-acceptor	3.12	-1.2
	6-ring	CA SER 90 (C)	pi-H	4.21	-1.0
3T88	O 29	ND2 ASN 107 (E)	H-acceptor	2.96	-2.5
	6-ring	CD LYS 54 (E)	pi-H	4.08	-1.0

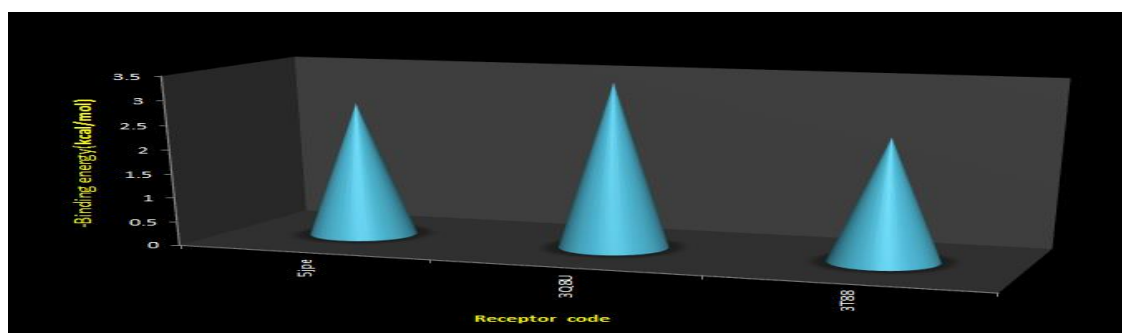


Figure. 5: Binding energy of L Schiff base with different protein receptors.

Conclusions

The newly synthesized L ligand was prepared as divalent and trivalent metal complexes. With the help of two imine nitrogen, the Schiff base L functioned as a neutral bidentate ligand. Following a thorough characterization of the complexes, it was observed that all chelates displayed greater biological activity than the free ligand. The antibacterial behavior of ligands is thus significantly impacted by metal chelation. In light of the chelation principle, the antibacterial activity was clearly demonstrated. Among the produced complexes, the Co(II) complex can be regarded as the most promising, powerful, and all-purpose antibacterial chemical. The synthesized compounds' antifungal efficacy demonstrated Co(II) and Ni(II) outstanding activity. Comparing the Mn(II) complex to the HepG2 cancer cell line, more anticancer activity was seen. Greater anticancer activity was shown by the Ni(II) complex against the PC3 cancer cell. Of all the produced compounds, the Cr(III) complex demonstrated the highest antioxidant activity. The synthetic chemicals' biological activity shows promise, but more extensive research on both humans and animals is still needed.

Conflicts of interest

There are no conflicts to declare.

References

1. Y. Li, Z.S. Yang, H. Zhang, B.J. Cao, F.D. Wang, *Bioorg. Med. Chem.* 11 (2003) 4363-4368.
2. M.J. O'Donnell, *Acc. Chem. Res.* 37 (2004) 506-517.
3. S. Rana, S.K. Mittal, N. Singh, J. Singh, C.E. Banks, *Sens. Actuators B Chem.* 239 (2016) 17-27.
4. G. Yuan, Y. Tian, J. Liu, H. Tu, J. Liao, J. Yang, Y. Yang, D. Wang, N. Liu, *Chem.Eng. J.* 326 (2017) 691-699.
5. Z.L. You, H.L. Zhu, *Z. Anorg. Allg. Chem.* 630 (2004) 2754-2760.
6. X. Liu, C. Manzur, N. Novoa, S. Celedon, D. Carrillo, J.R. Hamon *Coord. Chem. Rev.* 357 (2018) 144-172.
7. V. Alexander, *Chem. Rev.* 95 (1995) 273-342.
8. C.M. Silva, D.L. Silva, L.V. Modolo, R.B. Alves, M.A. Resende, C.V.B. Martins, A. Fatima, *J. Adv. Res.* 2 (2011) 1-8.
9. A. M. Fathi, H. S. Mandour, H. Anouar, *J Mol Struct* (2020).
10. Ijahdali, M., El-Sherif, A.A., Shoukry, M.M. *J Solution Chem* 42, 1028–1050 (2013). <https://doi.org/10.1007/s10953-013-0015-9>
11. Ahmed A. Soliman, Mina A. Amin, Ahmed A. El-Sherif, Cigdem Sahin, Canan Varlikli, *Arabian Journal of Chemistry*, Volume 10, Issue 3, (2017) Pages 389-397.
12. G.A.M Elhagali, G.A Elsayed, R.A. Eliswey, A.A. El-Sherif, *J Iran Chem Soc*15 (2018) 1243-1254.
13. E.S. Mousa, W.H. Mahmoud, *A. Organometal Chem* 33 (2019) e4844.
14. A. I. Vogel, *Quantitative Inorganic Analysis Including Elemental Instrumental Analysis*, 2nd ed., Longmans; London, 1962.
15. A.T. Abdelkarim, W.H. Mahmoud, A.A. El-Sherif, *J Mol Liq.* 328 (2021) 115334.
16. Albert, A., *Selective Toxicity*, Wiley: New York, 1979. Bakir Jeragh, Dhuha Al-Wahaib, Ahmed A. El-Sherif, and Ali El-Dissouky, *Journal of Chemical & Engineering Data* 52 (5), (2007), 1609-1614.
17. S. Chandra, D. Jain, A. K. Sharma, P. Sharma, *Molecules* 14 (2009) 174-190..
18. K.A. Asla, A.T. Abdelkarim, G.M.A El-Reash, A.A. El-Sherif, *Int J Electrochem Sci.* 15 (2020) 3891-3913.
19. P. Skehan, R. Storeng, A. Scudiero, J. Monks, D. McMahon, J.T. Vistica, H. Warren, S. Bokesch, M.R. Kenney, J. Boyd. *Nat. Cancer Inst.* 82 (1990) 1107.
20. A.A. El-Sherif, M.M. Shoukry, A.T. Abd Elkarim, M.H. Barakat, *Bioinorg Chem Appl*,2014 (2014) 626719.
21. M. M Abd-Elzaher, A. A. Labib, H. A. Mousa, S. A. Moustafa, M. M. Ali, A. A El-Rashedy, *J. Bas. App. Sci.* 5 (2016) 85.
22. A.A. El-Sherif, M.R. Shehata, M.M. Shoukry, N.M. Mahmoud, *J Mol Liq.* 262(2018) 422-434
23. A.A. El-Sherif, A. Fetoh, Y.Kh. Abdulhamed, G. M. Abu El-Reash, *Inorg Chim. Acta* 480 (2018) 1–15.

23. D. D. Patel, K. R. Patel, *Proceedings* (2021), *Materials today*.
24. M.S. Aljahdali, A.A El-Sherif, *Bioinorg Chem Appl*, 2020 (2020), 8866382.
25. A.A. El-Sherif, A.A El-Sisi, M. Ali, O. AlTaweel, A.T AbdEl-Karim, *Int J Electrochem Sci*. 15 (2020) 10885-10907.
26. J. Zhang, L. Xu, W. Wong, *Coord. Chem. Rev.* 335 (2018) 180-198.
27. A. Rambabu, N. Ganji, S. Daravath, K. Venkateswarlu, K. Rangan, Shivaraj, *J Mol. Str.* 1199 (2020) 127006.
28. M. Hong, G. Chang, R. Li, M. Niu, *New J. Chem.* 40 (2016) 7889-7900.
29. A. Rambabu, M.P. Kumar, S. Tejaswi, N. Vamsikrishna, Shivaraj, *J. Photochem. Photobiol. B Biol.* 165 (2016) 147-156.
30. W. H. Mahmoud, R. G. Deghadi, G. G. Mohamed, *India. J. Chem.* 58 (2019) 1319.
31. S.B. Bukhari, S. Memon, M. Mahroof-Tahir, M.I. Bhanger, *Spectrochim. Acta Part A Mol. Biomol. Spectrosc.* 71 (2009) 1901-1906.
32. J. Gabrielska, M. Soczyńska-Kordala, J. Hładyszowski, R. Żyłka, J. Miśkiewicz, S. Przystański, *J. Agric. Food Chem.* 54 (2006) 7735-7746.
33. M.-H. Shih, F.-Y. Ke, *Syntheses and evaluation of antioxidant activity of sydnonyl substituted thiazolidinone and thiazoline derivatives*, *Bioorg. Med. Chem.* 12 (2004) 4633-4643.
34. E. Üstün, M. Çolayvaz, M. Çelebi, S. D. Gizem, I. Özdemirb, *Inorg. Chim. Acta* (2016), 450, 182.
35. A. Y. Al-Dawood, N. M. El -Metwaly, H. A. El-Ghamry, *J. Mol.Liq.* (2016), 220, 311.
36. R. Zaky, A. Fekri, Y. G. Abou El-Reash, H. M. Youssef, A. Y. Kareem, *Egy. J. Basic and App. Sci.* (2016), 3, 272.
37. H. Kargar, V. Torabi, A. Akbari, R. Behjatmanesh-Ardakani, A. Sahraei, M. N. Tahir, *J Mol Str* 1205 (2020) 127642.
38. G. Ramesh, S. Daravath, M. Swathi, V. Sumalatha, D.S. Shankar, *Chem Data Coll* 28 (2020) 100434.
39. I. Belkhattab, S. Boutamine, H. Slaouti, M.F. Zid, H. Boughzala, Z. Hank, *J Mol Struct.* 1206 (2020) 127597.
40. C. Justin Dhanaraj, M. Jebapriya, C.J. Dhanaraj, M. Jebapriya, *J Mol. Struct.* 1220 (2020) 128596.
41. A. Chaudhary, R.V. Singh, *Phosphorus, Sulfur, Silicon Relat. Elem.* 178 (2013) 603-613.
42. B.G. Tweedy, *Plant extracts with metal ions as potential antimicrobial agents*, *Phytopathology* 55 (1964) 910-991.
43. S.E. Abd El-Razek, S.M. El-Gamasy, M. Hassan, M. S. Abdel-Aziz, S.M. Nasr, *J Mol Str* 1203 (2020) 127381.
44. M. Jafari, M. Salehi, M. Kubicki, A. Arab, A. Khaleghian, *Inorg. Chim. Acta*, 462 (2017) 329-335.
45. A.A. El-Sherif, M.M. Shoukry, L.O Abobakr, *Spectrochim Acta A Mol Biomol Spectrosc.* 112(2013) 290-300.
46. L. A. Anthony, D. Rajaraman, M. Shanmugam, K. Krishnasamy, *Chem. Data.* ISSN 1878-5352.